Power Limitation Control for a PMSG-Based Marine Current Turbine at High Tidal Speed and Strong Sea State

Zhibin Zhou, Franck Scuiller, Jean Frédéric Charpentier, Mohamed Benbouzid and Tianhao Tang

***Abstract*—This paper deals with the control strategies for a fixed-pitch marine current turbine (MCT) when the marine current speed exceeds the rated value corresponding to the rated power of generator and converter. Over-rated marine currents occur at large spring tides or under strong sea states; in these cases maximum power point tracking (MPPT) strategies must be changed to power limitation strategies for limiting the generator power at rated value. In this paper, two power limitation strategies with flux-weakening control are investigated. A feedback flux-weakening control is applied to extend the rotor speed operating range over the nominal MPPT tracking speed during high speed marine currents. In the speed control strategy, the turbine power characteristics are used to generate the rotor speed reference and the power limitation can be obtained at steady-state. In the torque control strategy, the generator torque is directly calculated by the power limitation and the rotor speed; this method enables to control the generator power at the limited value at dynamic process. Both strategies are investigated and compared at high tidal speeds without and with swell effect.**

***Index Terms*—Marine current turbine, power limitation, flux-weakening, torque control, swell effect.**

I. Introduction

Due to high predictability of the marine tides and high power potential of marine tidal currents, various turbine technologies have been developed to capture kinetic energy from marine tidal currents [1]. Some similar principles in wind generation systems can be applied in marine current turbine (MCT) systems due to the fact that both of them aim to capture energy from flowing mass. However, accessibility difficulties for underwater equipments make compact structure and low maintenance requirement highly expected for MCTs. Recent MCTs such as the OpenHydro (tested by French utility company EDF) and Alstom Hydro Beluga 9 adopt fixed blades to simplify the turbine system and use low speed permanent magnet synchronous generator (PMSG) to realize direct-drive conversion system.

The rated MCT power will not be designed for the peak marine current speed due to the reason that the peak current speed may happen only at large spring tides and corresponds only to a very small part of the statistical resource [2]. When the marine current speed is higher than the rated value, a fixed-pitch MCT is not able to limit the extracted power by pitch control as in SeaGen MCT turbine [3]. Therefore, an appropriate generator-side control strategy should be applied to limit the turbine and generator power.

Z. Zhou, F. Scuiller and J.F. Charpentier are with the French Naval Academy, IRENav EA 3634, 29240 Brest Cedex 9, France (e-mail: zhibin.zhou@ecole-navale.fr, Franck.Scuiller@ecole-navale.fr, Jean-Frederic.Charpentier@ecole-navale.fr,). Z. Zhou is also with the University of Brest and the Shanghai Maritime University.

M.E.H. Benbouzid is with the University of Brest, EA 4325 LBMS, Rue de Kergoat, CS 93837, 29238 Brest Cedex 03, France (e-mail: Mohamed.Benbouzid@univ-brest.fr).

T. Tang is with the Shanghai Maritime University, 201306 Shanghai, China (email: thtang@shmtu.edu.cn).

This work is supported by Brest Métropole Océane (BMO).

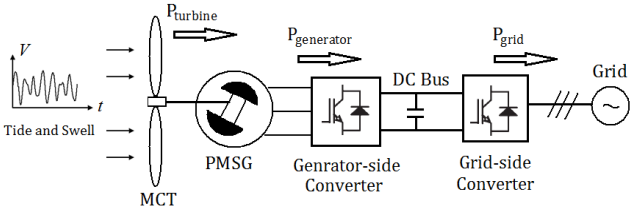

Fig. 1. General scheme for a PMSG-based MCT system.

In this paper, a 1.5 MW PMSG-based MCT system is studied. Figure 1 shows the general system scheme, and the generator-side control will be focused. A flux-weakening method proposed in [4-5] is chosen to enable the PMSG to operate in over-rated speed for realizing power limitation control at high marine current speeds. Two power limitation control strategies (speed control strategy and torque control strategy) are proposed. Their performances are compared both in steady-state and dynamic state (considering strong sea state with swell effects).

In Section II, the turbine power characteristics and the generator model are described. In Section III, the flux-weakening control and two power limitation strategies are presented. In Section IV, simulation results of the two power limitation strategies at high tides with and without swell effect are illustrated and compared. The conclusion is then given in Section V.

II. Marine Current Turbine and Generator Model

A. Marine Current Turbine Model

For MCTs, the power extracting principles are similar to wind turbines. The power harnessed by a horizontal-axis MCT can be calculated by the following equation.

$$P = \frac{1}{2}\rho C_p \pi R^2 V^3 \qquad (1)$$

In (1), the sea water density ρ and the turbine radius R are considered as constants; V is the marine current speed which is considered to be homogeneous in the turbine disk for each given time; C_p is the turbine power coefficient which depends on the turbine blade structure and its hydrodynamics. For typical MCTs, the optimal C_p value for normal operation is estimated to be in the range of 0.35-0.5 [2]. For a given

turbine and based on the experimental results, the C_p curve can be approximated as a function of the tip speed ratio ($\lambda = \omega_m R / V$) and the pitch angle [7]. In this paper the considered system is a fixed pitch MCT, so C_p depends only of λ .

Figure 2 shows the C_p curve used in this paper. The maximum C_p value is 0.45 which corresponds to a tip speed ratio of 6.3. This value is considered as the optimal tip speed ratio (λ_{opt}) for realizing maximum power point tracking (MPPT) under rated marine current speeds.

In this paper, a 1.5 MW direct-driven turbine with 8 m of radius is studied. The turbine maximum speed to follow MPPT is 25 rpm (2.62 rad/s) for a marine current of 3.2 m/s. When the marine current exceeds 3.2 m/s, the extracted power will be limited to 1.5 MW by power limitation strategies with flux-weakening control. The MCT extractable power under different marine current speeds is calculated by (1) and illustrated by Fig. 3. For marine current speed lower than 3.2m/s, a modified MPPT strategy with filter algorithm to utilize system inertia for reducing power fluctuations under swell disturbance will be used. This method has been investigated in the previous work [8]. In this paper we will focus on the power limitation control stage at over-rated marine current speeds.

B. Marine Current Generator Model

The PMSG dynamic model is given in a synchronous rotation *d-q* frame. Equation (2) shows the Park transform used in the generator side part. The *d*-axis is oriented to the rotor flux axis and θ is the electrical angle between the stator phase *a* axis and the *d*-axis.

$$\begin{bmatrix} v_d \\ v_q \end{bmatrix} = \frac{2}{3} \begin{bmatrix} \cos\theta & \cos\left(\theta - \frac{2\pi}{3}\right) & \cos\left(\theta + \frac{2\pi}{3}\right) \\ -\sin\theta & -\sin\left(\theta - \frac{2\pi}{3}\right) & -\sin\left(\theta + \frac{2\pi}{3}\right) \end{bmatrix} \begin{bmatrix} v_a \\ v_b \\ v_c \end{bmatrix} \quad (2)$$

The PMSG model in the *d-q* frame can be described by the following equations ($L_d = L_q$ in this paper which corresponds to a non-salient machine).

$$\begin{cases} v_d = R_s i_d + L_d \frac{di_d}{dt} - \omega_e L_q i_q \\ v_q = R_s i_q + L_q \frac{di_q}{dt} + \omega_e L_d i_d + \omega_e \psi_m \\ T_e = \frac{3}{2} n_p \psi_m i_q \\ J \frac{d\omega_m}{dt} = T_m - T_e - f_B \omega_m \end{cases} \quad (3)$$

In (3), v_d , v_q and i_d , i_q are stator voltages and currents in the *d-q* frame respectively; R_s is the stator resistance; L_d , L_q are inductances in the *d-q* frame; ω_e , ω_m are machine electrical and mechanical speed; T_e , T_m are respectively the machine electro-magnetic torque and the turbine mechanical torque; n_p is the machine pole pair number; ψ_m is the flux linkage created by the rotor permanent magnets; J is the total system inertia and f_B is the friction coefficient associated to the mechanical drive train.

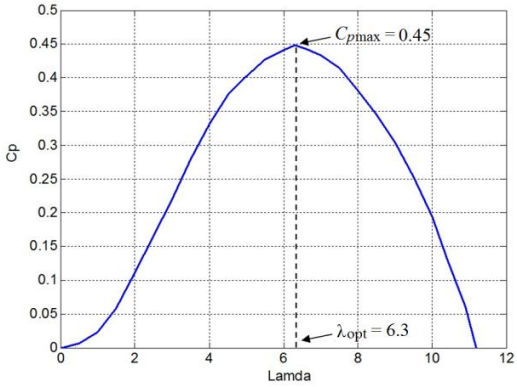

Fig. 2. C_p curve of the MCT.

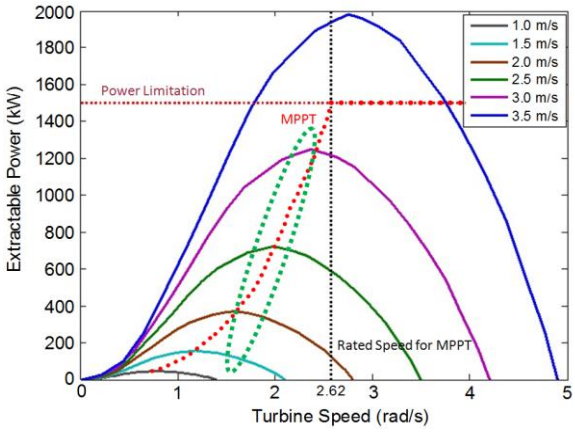

Fig. 3. The MCT extractable power.

III. Power Limitation Control with Flux-weakening

A. Flux-weakening Control

In the synchronous rotation frame, the stator current is decomposed to flux component i_d and torque component i_q ; and the following voltage and current limits must be guarantied at any time.

$$v_d^2 + v_q^2 \le V_{max} \quad (4)$$

$$i_d^2 + i_q^2 \le I_{max} \quad (5)$$

In (4) and (5), V_{max} is the maximal available phase voltage magnitude and I_{max} is the maximal phase current magnitude. V_{max} is determined by the available DC-link voltage V_{dc} and the converter modulation method. $V_{max} = 1/\sqrt{3}\, V_{dc}$ for the sinusoidal wave model (linear space vector modulation) and $V_{max} = 2/\pi\, V_{dc}$ for the full six-step operation [5]. I_{max} is determined by machine and converter power ratings.

For a surface-mounted PM machine, the inductances in *d*-axis and *q*-axis are almost equal ($L_d = L_q = L_s$). By neglecting stator resistance, the voltage limitation equation (4) in steady-state can therefore be expressed by

$$i_q^2 + \left(i_d + \frac{\psi_m}{L_s} \right)^2 \le \left(\frac{V_{max}}{\omega_e L_s} \right)^2 \quad (6)$$

From (5) and (6), The voltage and current limitation circles can be drawn as shown in Fig. 4 ($\omega_1 > \omega_2 > \omega_3 > \omega_4$). The solid-line circle indicates the current limitation with I_{max} as the radius. The dotted-lines indicate voltage limitation circles which have a centre of (0, $-\psi_m/L_s$) and will shrink with the increase of the operating speed.

The typical control strategy for non-salient PM machine at low speeds is to set $i_d = 0$ for maximizing the torque per ampere ratio. At high speeds over the machine base speed, the voltage limitation circle may shrink to the left side of the *q*-axis in Fig. 4 and that indicates negative *d*-axis current should be injected to decrease the total flux in the machine windings. The operating points above the base speed should always be within the voltage limit circle. It should be noticed that the maximum torque in the flux-weakening operation is obtained when the PMSM operates at the cross-points of the voltage and current limitation circles. The cross-points shown in Fig. 4 can be calculated when the equality sign is used in (5) and (6); and then the corresponding reference i_d and the corresponding i_q for maximum torque available in the flux-weakening stage can be obtained as follows.

$$i_d^* = \frac{L_s}{2\psi_m} \left[\left(\frac{V_{max}}{\omega_e L_s} \right)^2 - \left(\frac{\psi_m}{L_s} \right)^2 - I_{max}^2 \right] \quad (7)$$

$$\left| i_q \right|_{max} = \sqrt{I_{max}^2 - i_d^{*2}} \quad (8)$$

From (7) , it can be seen that the model-based *d*-axis current reference requires accurate information about machine parameters and operating speed. Therefore, robust flux-weakening methods are more favorable in real applications. In this paper, the method proposed in [4-5] is chosen to generate *d*-axis current reference at over base speed operation. In this paper, the flux-weakening is operating to limit the generator power at rated constant power. It means that the corresponding steady state operating points are situated under the limits defined by (7) and (8).

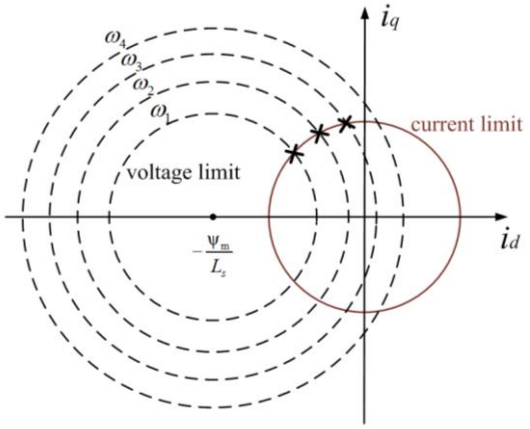

Fig. 4. Voltage and current limitation circles.

Figure 5 illustrates the generator-side control scheme with flux-weakening algorithm for realizing high speed operation at MCT power limitation stage. The difference between the current controller output (voltage reference) and the converter output voltage (real machine voltage) is used to produce the i_d reference. The low past filter (LPF) is capable of rejecting high-frequency components in the voltage signals and thus high-frequency oscillation in the i_d reference can be avoided. The converter output voltage is limited by the DC-link voltage, and this control scheme enables to maximize the DC-link voltage utilization while maintaining the current control capability. The i_q reference is given by required torque and limited by (8). The MCT required torque can be obtained by speed control strategy or torque control strategy, which will be discussed in the followed sections.

B. Speed Control Strategy

In a speed control strategy, the rotor speed is directly controlled and the generator torque reference or the i_q reference signal is obtained from the output of speed loop controller. Supposing that the C_p curve is known and the

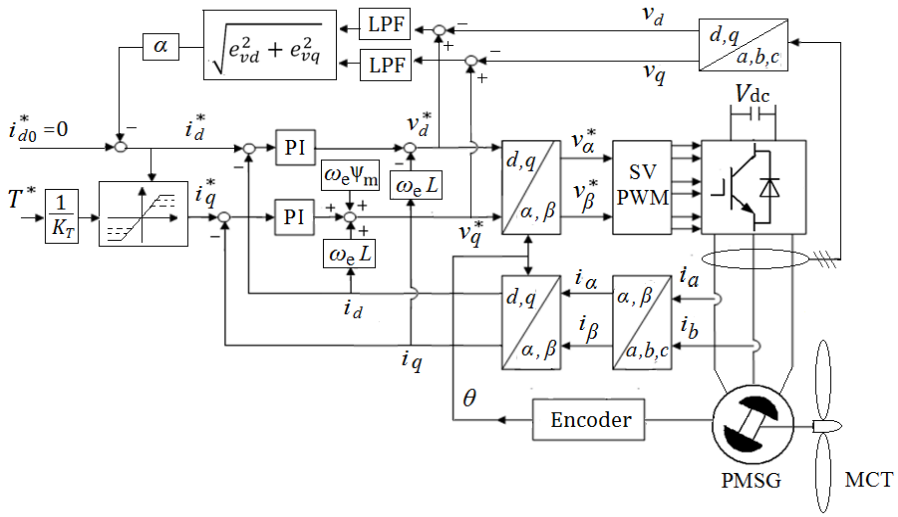

Fig. 5. Flux-weakening control scheme for the generator-side converter.

marine current speed V can be obtained by flow velocity measurements, the rotor speed should be controlled to keep the turbine tip speed ratio at λ_{opt}, thus keeping the turbine power coefficient C_p at the maximum value when the marine current speed is below the rated value. A modified tip speed ratio based MPPT with filter algorithm is proposed in the previous work as follows [8].

$$\omega_{m\_ref} = \frac{1}{Ts+1} \cdot \frac{\lambda_{opt} V}{R} \tag{9}$$

where the T is the filter time constant and plays a significant role in reducing the generator power fluctuation at dynamic operation (acceleration/deceleration) in case of swell waves.

When the marine current speed is over the rated value, the MPPT mode must be changed to power limitation mode. In this case, the rotor speed reference can be calculated from the turbine power characteristics. The proposed rotor speed reference at power limitation mode is shown by Fig. 6. In this scheme: the required C_p value is first calculated by the generator power limitation (P_{limit}) and the marine current speed V based on the turbine power equation (1), the corresponding tip speed ratio is then obtained based on the right part of the C_p curve ($\lambda > \lambda_{opt}$). In this way, the generator power can be controlled to the limited value for a given over-rated marine current speed in the steady-state. The filter in Fig. 6 is used for avoiding rapid acceleration/deceleration, especially necessary in case of strong sea state.

The speed control strategy relies on the information of marine current speed and turbine power characteristics. It should be noticed that the generator power will equal the turbine power at steady-state.

B. Torque Control Strategy

In order to directly control the generator power at power limitation stage, a torque control strategy can be applied. At high current speed, the generator torque reference can be calculated by dividing the limitation power with rotor speed ($T_{ref} = P_{limit} / \omega_m$). In this way, the generator torque will be controlled to keep the generator power at the limitation value. Torque control strategy does not require the marine current speed and turbine power characteristics information; it is simple and fast for realizing the power limitation requirement. When the marine current speed is under the rated value, a torque-based MPPT strategy can be applied [9]. This torque-based MPPT (also called optimal torque control) calculates the reference generator torque as a function of C_{pmax}, λ_{opt} and ω_m.

The (10) illustrates the proposed torque control strategy in both MPPT stage and power limitation stage. In (10), T_{ref_max} is the maximum generator torque which can take the value of generator rated torque. The switch of the torque reference between MPPT mode and power limitation mode can also be

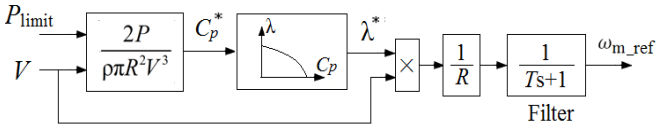

Fig. 6. Rotor speed reference at power limitation mode.

$$T_{ref} = \begin{cases} T_{ref\_MPPT} = \dfrac{1}{2} \dfrac{C_{p\max}}{\lambda_{opt}^3} \rho \pi R^5 \omega_m^2 \;,\; T_{ref\_MPPT} \le T_{ref\_max} \\ T_{ref\_power\_limit} = \dfrac{P_{limit}}{\omega_m} \;,\; T_{ref\_MPPT} > T_{ref\_max} \end{cases} \tag{10}$$

triggered by comparing the real rotor speed and the rated rotor speed.

IV. Comparison of the Two Power Limitation Methods at High Speed Marine Currents

A. Under High Tidal Speed

In this case, the sea is supposed to be calm (without significant swell waves). The MCT is supposed to be installed at a proper depth under the sea-surface so that normal sea waves generated by local winds will have negligible influence for the MCT system. In this case,, high marine current speed is caused only by strong tidal current at spring tides. It should be noticed that tidal current speed is highly predictable for a given site.

Figure 7 gives an example of tidal current speed in the Raz de Sein (potential site for MCT project off the coast of Brittany, France) during one month based on tidal current data from SHOM (French Navy Hydrographic and Oceanographic Service). It can be seen that peak tidal speed can reach 3.6 m/s for this site. Without power limitation control, the maximum extractable power at the peak tidal speed would be over 2 MW for the MCT.

In the simulation, the marine current speed is initially set at 2.8 m/s and rises to 3.6 m/s during 20 s to 70 s as shown in Fig. 8. After 45 s, the current speed rises over the rated value (3.2 m/s) and the power limitation control strategy should be applied. Although this current speed rising process is not very realistic (the tidal speed changes very slowly in reality because a tidal cycle may correspond to approximately half a day), it enables to test the performances of the two power limitation strategies at high spring tides.

The turbine speed response, generator torque and power responses under the speed control and torque control strategies are illustrated respectively in Fig. 9 to 11. The system parameters can be found in Appendix and the maximum generator torque is limited at 600 kN·m.

It can be seen that after 45 s when the current speed rises over the rated value (3.2 m/s) and the generator torque will reach to its maximum value and the power limitation mode will be triggered in both speed control and torque control

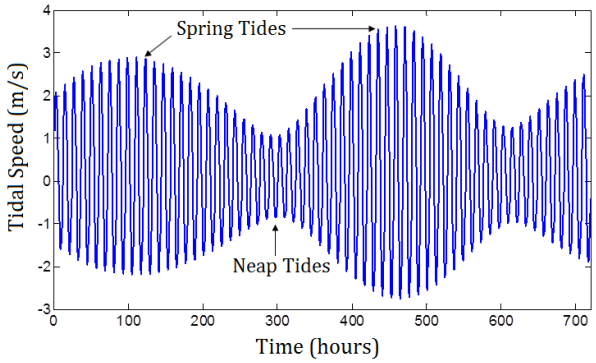

Fig. 7. Tidal speed in the Raz de Sein for one month [2].

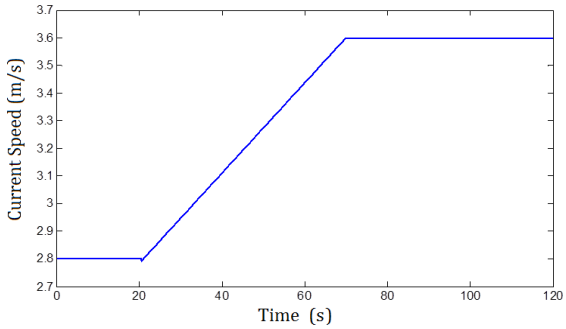

Fig. 8. High tidal speed.

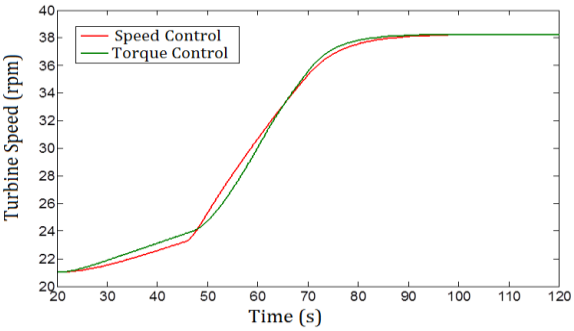

Fig. 9. Turbine speed responses at high tidal speed.

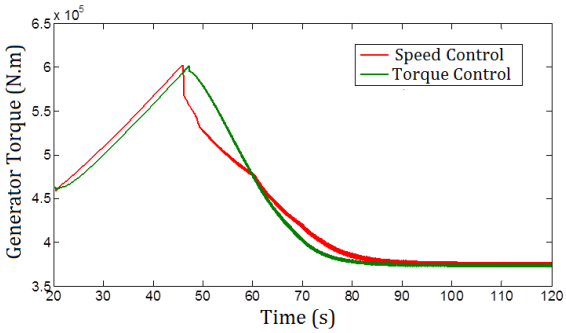

Fig. 10. Generator torque responses at high tidal speed.

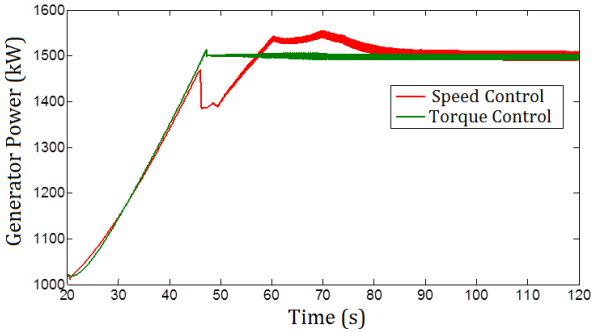

Fig. 11. Generator produced power responses at high tidal speed.

strategies. The decrease of the generator torque with the rise of the rotor speed over the rated speed (25 rpm) shown in Fig. 9 and 10 indicates that the flux-weakening control works well in both power limitation control strategies. From Fig. 10 and 11, the deeper drop of generator torque and power can be observed in speed control at the beginning of the over-rated current speed. This indicates that the speed control strategy tries to fast accelerate the MCT at power limitation mode based on the turbine power characteristics. At steady-state when the marine current equals to the peak value (3.6 m/s), both control strategies can limit the generator power to the limitation value of 1.5 MW. During transient high current speed stage, only the torque control strategy enables the generator power to be controlled at 1.5 MW; the speed control strategy fails to do that due to the generator power is not directly controlled.

B. Under Swell Effect

In this part, the swell effect which may cause marine current speed to be over the rated value is taken into account. Swell refers to long-length ocean waves (usually over 150 m) generated from distant storms [10]. Long distance dispersion makes the swell spectrum narrower and the energy more accumulated than local wind-generated waves. Swells can propagate very deep below the sea surface and therefore have a non-negligible effect on the MCT system. Indeed, swell effect can lead to marine current speed fluctuations on a period about 10 to 20 s. The swell-induced marine current speed variations can be calculated based on location parameters (sea depth and turbine installation depth) and sea state. Swell effect modeling have been done in the previous work [8].

In this paper, a medium-strong sea state with significant wave height H_s = 3 m and typical wave period T_p = 13.2 s is considered. This corresponds to typical sea state in the winter for the western coast of Europe. The base tidal speed is set to 2.8 m/s and the total marine current speed is calculated as the sum of the tidal current speed and the swell-induced current speed variations. Figure 12 shows the marine current speed under swell effect. It can be seen that even the tidal current speed is fixed at 2.8 m/s, the total marine current speed will exceed the rated value of 3.2 m/s during some periods due to variations induced by swell effect.

Figure 13 and 14 show the turbine torque and generator torque responses with speed control and torque control respectively. The turbine torques in both control schemes seem quite similar; this indicates that the resulted power coefficient is similar in the proposed speed control and torque control scheme. However, the generator torques are different due to different control algorithms: the speed control triggers the power limitation mode at every moment when the marine current speed is over the rated value regardless the real generator power, while the torque control triggers the power limitation mode only when the generator power reaches to the limited value.

Figure 15 illustrates and compares the generator produced powers with the speed control and torque control strategies. It shows that torque control strategy is able to limit the PMSG

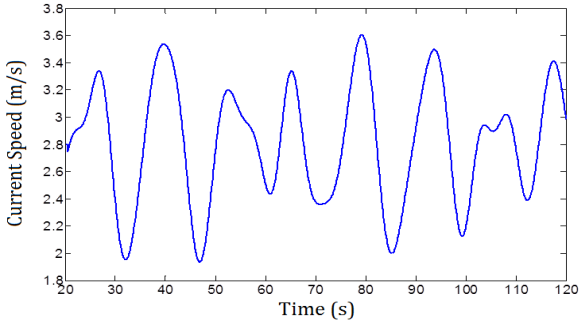

Fig. 12. Marine current speed under swell effect.

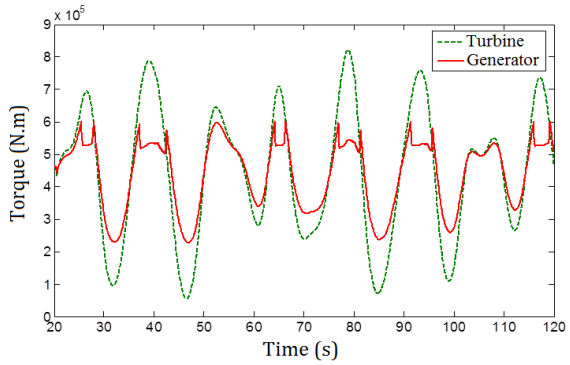

Fig. 13. Torque responses under swell effect with speed control strategy.

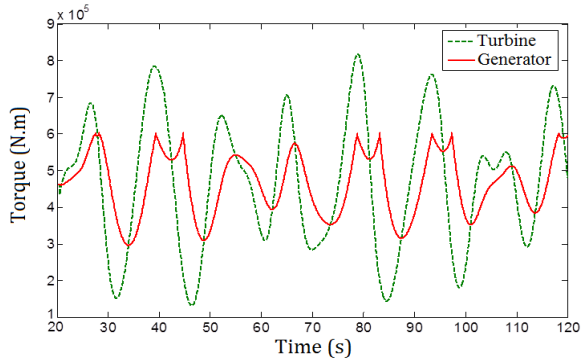

Fig. 14. Torque responses under swell effect with torque control strategy.

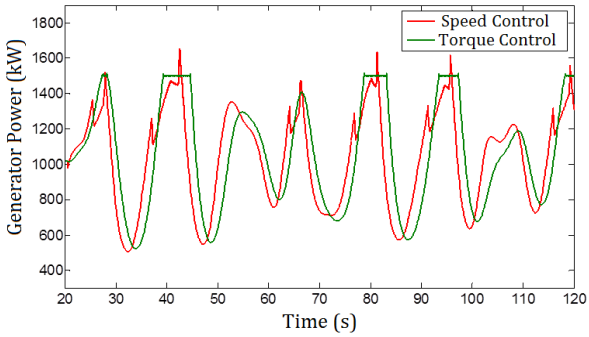

Fig. 15. Generator produced power responses under swell effect.

power to 1.5 MW more accurately than the speed control strategy at high marine current speed considering swell effect.

V. Conclusion

This paper investigates the power limitation control strategies for a PMSG-based MCT with non-pitchable blades when marine current speed exceeds the rated value. The power limitation idea is realized by accelerating the turbine to over-rated speed operating points and thus reducing the MCT extracted power. A robust flux-weakening control algorithm is selected to guarantee the over-rated speed operation of the PMSG. Two control strategies are proposed in this paper for obtaining the appropriate torque reference or *q*-axis current reference for generator-side power limitation control. At high marine current speed, the speed control strategy aims to control the power based on the turbine power characteristics, and the torque control strategy controls the generator torque directly based on the power limitation value and the rotor speed. Both strategies are studied at high tidal speed with and without swell effect. Simulation results show that both strategies are capable of limiting the generator produce power to the rated value at steady-state; torque control scheme works more efficiently than speed control scheme due to the fact that generator power is more directly controlled during dynamic stages.

Appendix

TABLE I
System Parameter List

Sea water density	1027 kg/m^3
Turbine blade radius	8 m
Maximum C_p value	0.45
Optimal tip speed ratio for MPPT	6.3
Rated marine current speed	3.2 m/s
System total inertia	1.3131×10^6 kg·m^2
Generator rated power	1.5 MW
Generator rated phase voltage	520 V (RMS)
Generator rated phase current	961.5 A (RMS)
DC-bus rated voltage	1500 V
Rotor rated speed	25 rpm
Pole pair number	120
Permanent magnet flux	2.458 Wb
Generator stator resistance	0.0081Ω
Generator *d-q* axis inductance	1.2 mH

References

[1] S. Benelghali, M.E.H. Benbouzid and J. F. Charpentier, "Marine tidal current electric power generation technology: State of the art and current status," *in Proceedings of the 2007 IEEE IEMDC*, Antalya (Turkey), vol. 2, pp. 1407-1412, May 2007.

[2] S. Benelghali, R. Balme, K. Le Saux, M.E.H. Benbouzid, J.F. Charpentier and F. Hauville, "A simulation model for the evaluation of the electrical power potential harnessed by a marine current turbine," *IEEE Journal on Oceanic Engineering*, vol. 32, n°4, pp. 786-797, October 2007.

[3] T. Thiringer, J. MacEnri, and M. Reed, "Flicker evaluation of the SeaGen tidal power plant," *IEEE Trans. Sustainable Energy*, vol. 2, n°4, pp. 414 –422, Oct. 2011.

[4] T. S. Kwon, and S. K. Sul, "Novel antiwindup of a current regulator of a surface-mounted permanent-magnet motor for flux-weakening control," *IEEE Trans. Industry Applications*, vol. 42, n°5, pp.1293-1300, Sep./Oct. 2006.

[5] T. S. Kwon, and S. K. Sul, "A novel flux weakening algorithm for surface mounted permanent magnet synchronous machines with infinite constant power speed ratio," *in Proceedings of the 2007 IEEE ICEMS*, Seoul (Korea), pp. 440-445, Oct. 2007.

[6] H. Liu, Z. Q. Zhu, E. Mohamed, Y. Fu, and X. Qi, "Flux-weakening control of nonsalient pole PMSM having large winding inductance, accounting for resistive voltage drop and inverter nonlinearities ," *IEEE Trans. Power Electronics*, vol. 27, n°2, pp.942-952, Feb. 2012.

[7] J.G. Slootweg, S.W.H. de Haan, H. Polinder and W.L. Kling, "General model for representing variable speed wind turbines in power system dynamics simulations," *IEEE Trans. Power Systems*, vol. 18, n°1, pp.144-151, February 2003.

[8] Z. Zhou, F. Scuiller, J.F. Charpentier, M.E.H. Benbouzid and T. Tang, "Grid-connected marine current generation system power smoothing control using supercapacitors," *in Proceedings of the 2012 IEEE IECON*, Montreal (Canada), pp. 4035-4040, Oct. 2012.

[9] S. Morimoto, H. Nakayama, M. Sanada, and Y. Takeda, "Sensorless output maximization control for variable-speed wind generation system using IPMSG," *IEEE Trans. Industry Applications*, vol. 41, n°1, pp. 60-67, Jan./Feb. 2005.

[10] Y. Goda, *Random Seas and Design of Maritime Structures*. Advanced Series on Ocean Engineering, vol.33, World Scientific: Singapore, 2010